Convection in Porous Media with Dispersion

Baole Wen,
Yu Liang, Marc Hesse, David DiCarlo

1. The Institute for Computational Engineering and Sciences (ICES),
   University of Texas at Austin, Austin, TX 78712 USA
2. Department of Geological Sciences, Jackson School of Geosciences,
   University of Texas at Austin, Austin, TX 78712 USA
3. Hildebrand Department of Petroleum and Geosystems Engineering

SIAM Annual Meeting,
Portland, Oregon, July 12, 2018

Funding from DOE Award DE-SC0001114 is gratefully acknowledged

U.S. DEPARTMENT OF ENERGY
Office of Science
CFSES
TEXAS
The University of Texas at Austin
ICES

Background: Geological CO_2 Storage

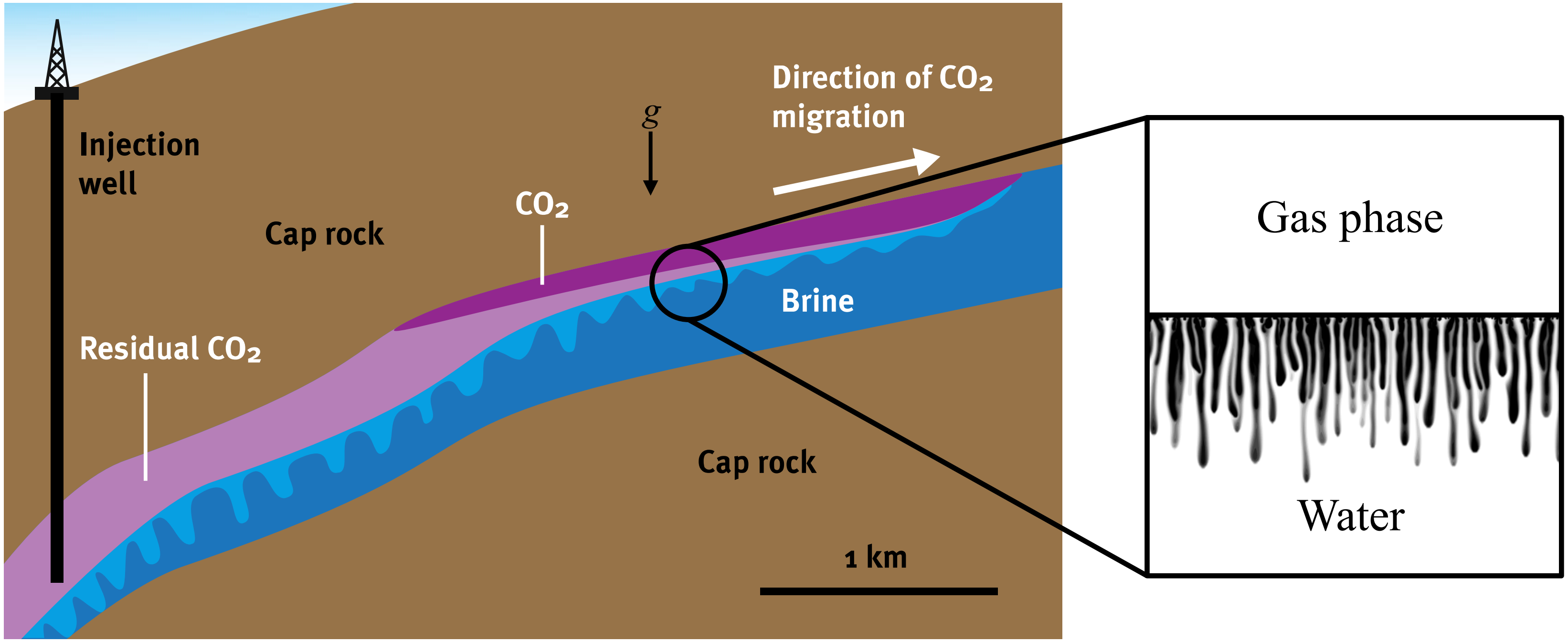

Schematic of the CO_2 sequestration process (Blunt, 2010)

- Geologic carbon storage in deep saline aquifers is a promising technology for reducing anthropogenic emissions into the atmosphere
- Dissolution of injected CO_2 into resident brines is one of the primary trapping mechanisms generally considered necessary to provide long-term storage security

Porous media convection at large *Ra* (previous studies)

Thermal convection (two-sided) — Solutal convection (one-sided)

$Ra = 10^4$

$Ra = 2 \times 10^4$

$Ra = 5 \times 10^4$

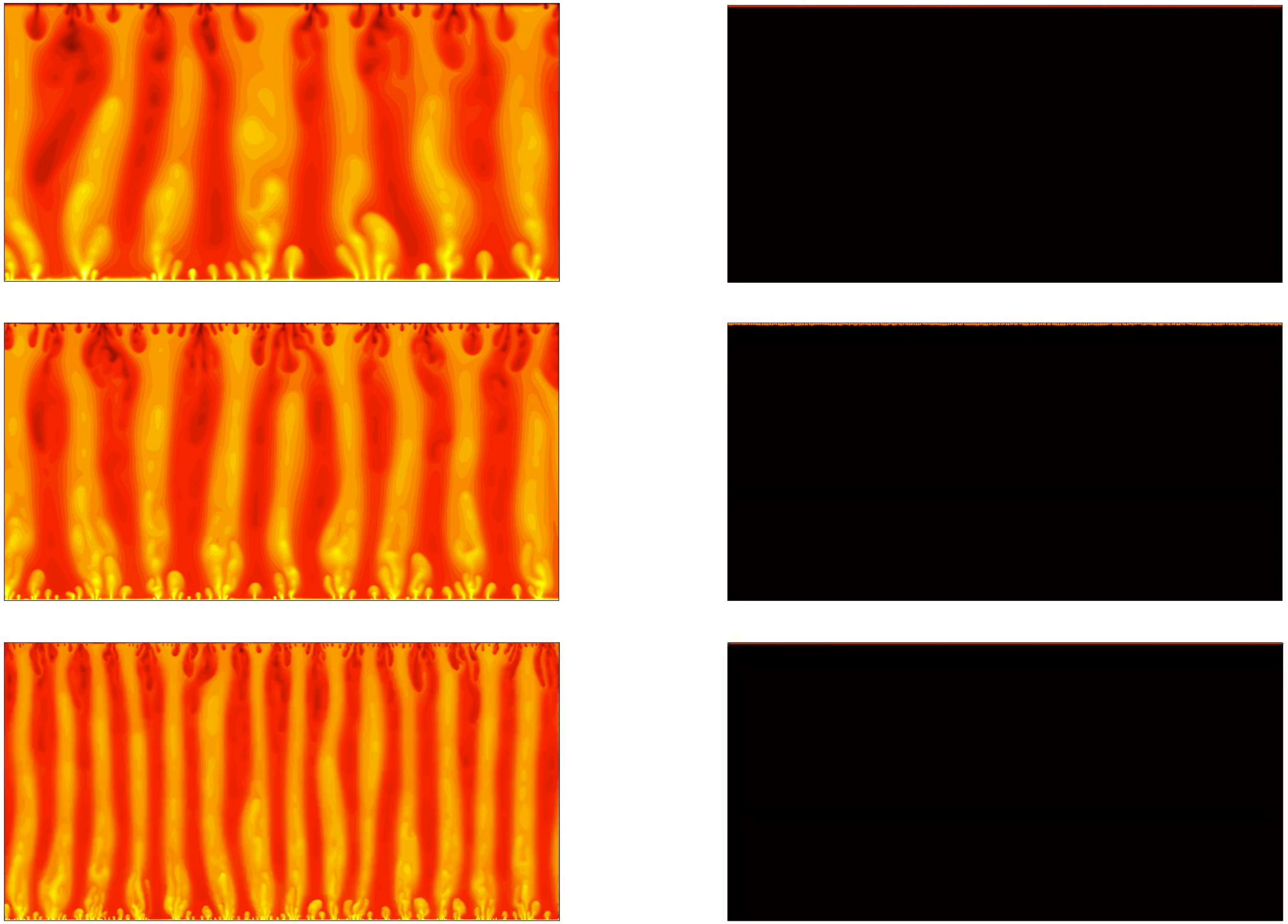

Note: the dynamics become ‘turbulent’ at $Ra > 1300$

- The inter-plume spacing $\delta \sim 1/Ra^{\alpha}$ with $\alpha \leq 0.5$; the flux $F \sim Ra$ (DNS, upper bounds)

Motivation & objective

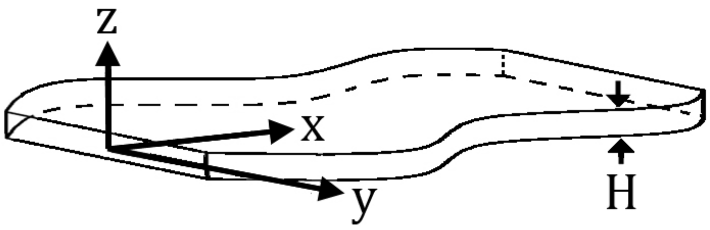

Hele-Shaw cell
(wikipedia)

$\approx$

but $\neq$

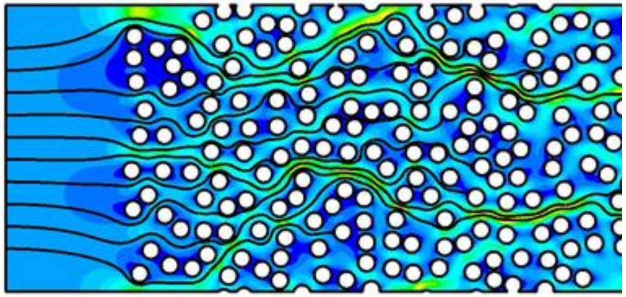

Flow through a porous medium
(www.comphys.ethz.ch)

Some problems for previous studies of porous media convection:

- Current laboratory experiments are generally performed in Hele-Shaw cells, which *lack* transverse mechanical dispersion
- Most numerical simulations *neglect* mechanical dispersion

We explore the pattern formation and transport properties of porous media convection by performing laboratory experiments in *granular* media and direct numerical simulations *with* mechanical dispersion

Experiments of solutal convection in *granular* media (Yu Liang)

Experimental setup: 2D analog fluid system, water + Methanol & Ethylene-Glycol (MEG)

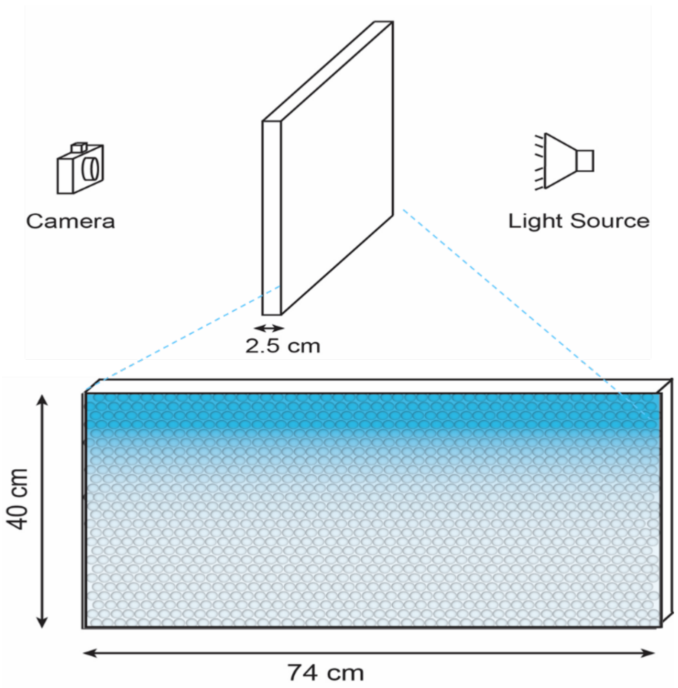

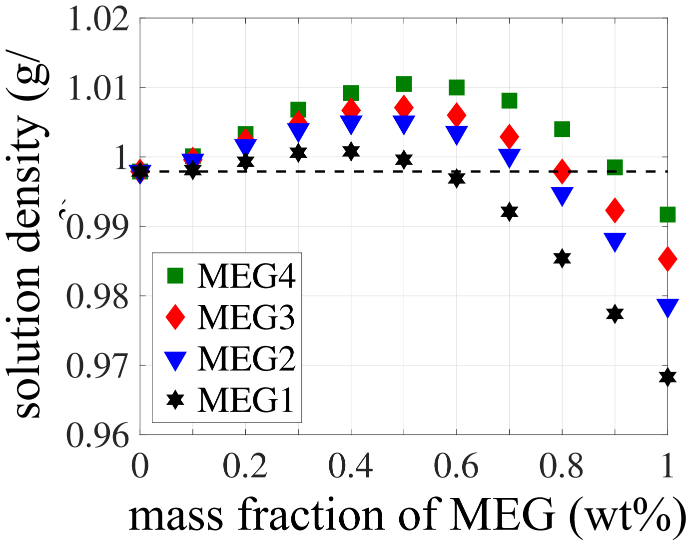

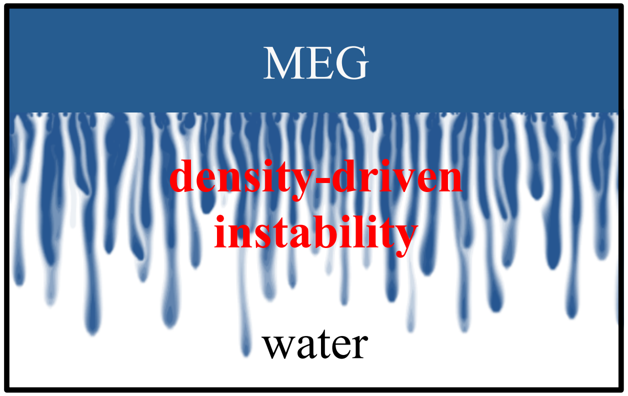

Parameters used in experiments:

(1) maximum density difference $\triangle\rho$:

0.0029, 0.0073, 0.0093, 0.0127 g/cm^3;

(2) diameter of glass beads d: 0.8, 1.2, 2, 3, 4 mm

Experimental results (1)

Processed images of two convective dissolution experiments with same MEG but different *d*

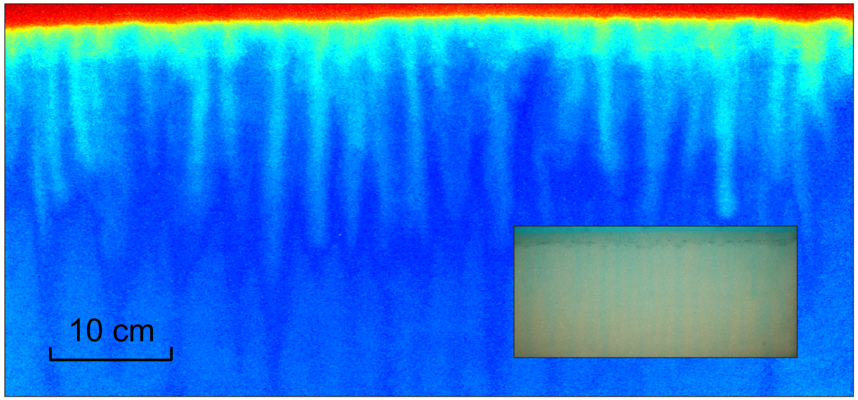

0.8 mm glass bead, $\triangle\rho = 9.3$ kg/m^3
$Ra_m = 1.4 \cdot 10^4$ (19 plumes)

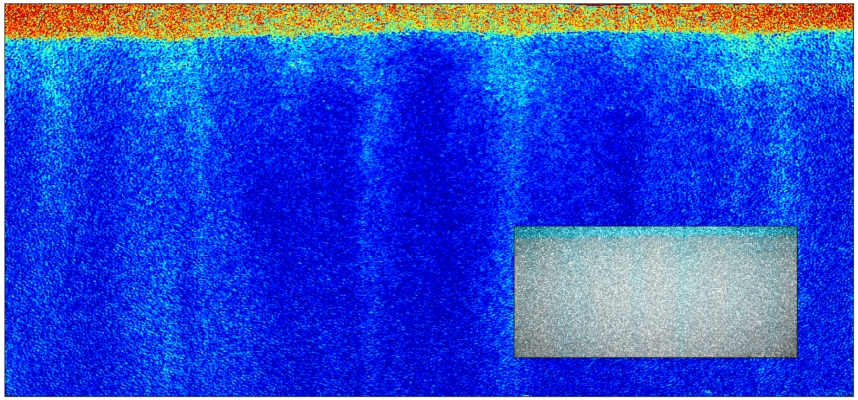

3 mm glass bead, $\triangle\rho = 9.3$ kg/m^3
$Ra_m = 2.1 \cdot 10^5$ (9 plumes)

Classical Rayleigh-Darcy number:

$$Ra_m = \frac{K \Delta \rho g H}{\mu \phi D_m}$$

Note: the medium permeability $K \sim d^2$

- A *larger* Rayleigh number *coarsens* the finger pattern, *contradicting* the classical prediction $\delta \sim 1/Ra^{\alpha}$ made in the absence of mechanical dispersion

Experimental results (2)

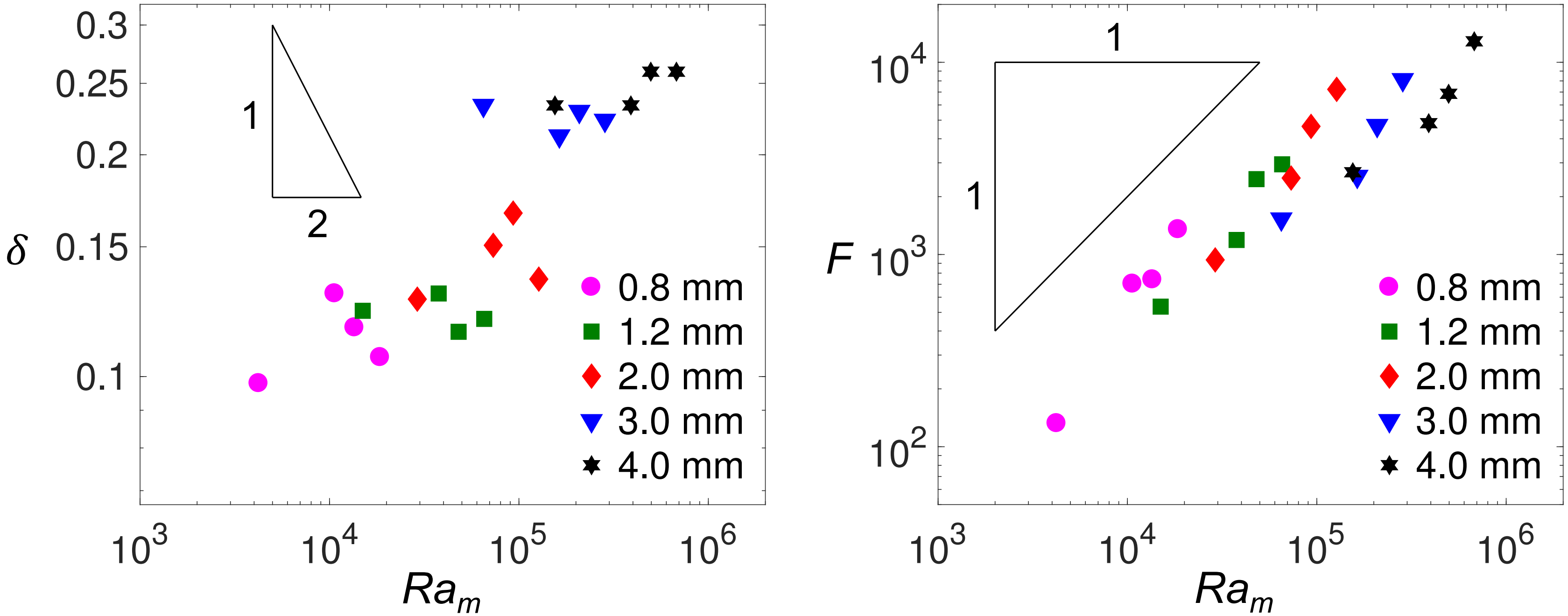

- Inter-plume spacing δ *increases* with Ra_m!
  Classical prediction: $\delta \sim 1/Ra_m^{\alpha}$

Note: $$Ra_m = \frac{K \Delta\rho g H}{\mu \phi D_m}$$

- Dissolution flux $F \sim c(d) \cdot Ra_m$ but with *different* prefactor c for various bead sizes

Classical prediction: $F \sim c \cdot Ra_m$ where c is constant

Hydrodynamic dispersion (Fickian model)

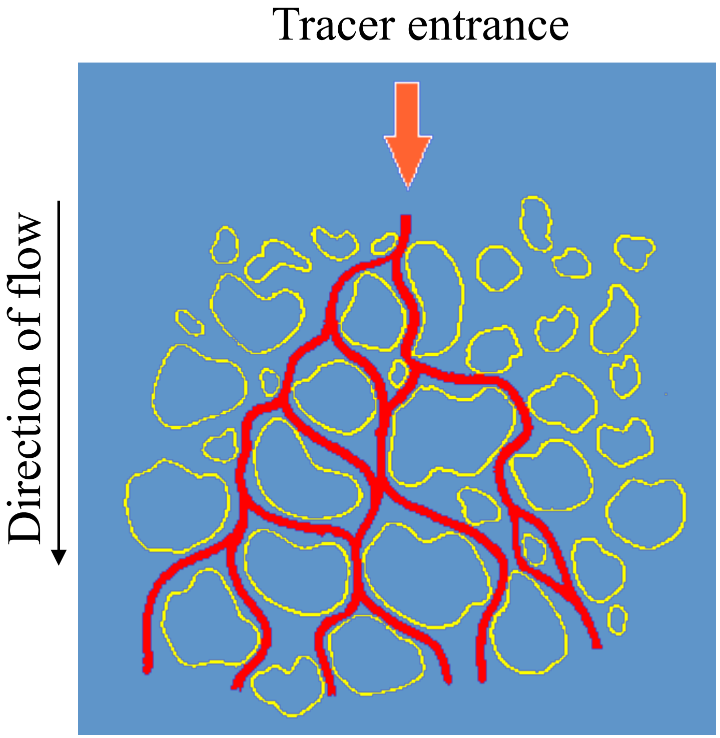

Tortuous flow paths in porous media that spread a tracer and create hydrodynamic dispersion

Dimensional mathematical formations:

$$\nabla^* \cdot \mathbf{u}^* = 0,$$
$$\mathbf{u}^* = -K/(\mu\phi)\,(\nabla^* P^* + \rho^* g \mathbf{e}_z),$$
$$\partial_{t^*} C^* + \mathbf{u}^* \cdot \nabla^* C^* = \nabla^* \cdot (\mathbf{D}^* \nabla^* C^*)$$

The hydrodynamic dispersion tensor (Fickian model) *along the flow streamline*:

molecular diffusion

mechanical dispersion

$$\begin{aligned}\mathbf{D}^* &= D_m \mathbf{I} + \boldsymbol{\alpha}|\mathbf{u}^*| \\ &= \begin{bmatrix} D_m^* & 0 \\ 0 & D_m^* \end{bmatrix} + \begin{bmatrix} \alpha_l |\mathbf{u}^*| & 0 \\ 0 & \alpha_t |\mathbf{u}^*| \end{bmatrix},\end{aligned}$$

where α_l and α_t are the longitudinal and transverse dispersivities, respectively.

In the fixed *Cartesian* reference frame:

$$\mathbf{D}^* = D_m \mathbf{I} + (\alpha_l - \alpha_t)\frac{\mathbf{u}^*\mathbf{u}^*}{|\mathbf{u}^*|} + \alpha_t |\mathbf{u}^*| \mathbf{I}$$

Non-dimensionalization and numerical method (2D)

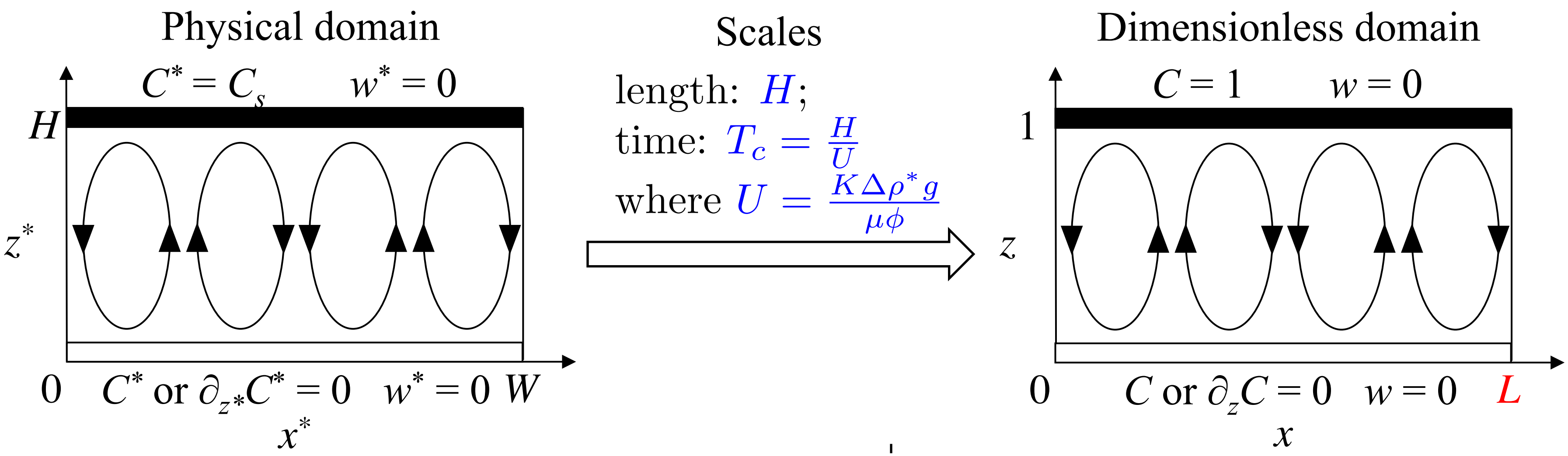

Scales

length: H;

time: $T_c = \frac{H}{U}$

where $U = \frac{K \Delta \rho^* g}{\mu \phi}$

$$\nabla \cdot \mathbf{u} = 0, \quad \mathbf{u} = -\nabla P - C\mathbf{e}_z,$$

$$\partial_t C + \mathbf{u} \cdot \nabla C = \nabla \cdot (\mathbf{D} \nabla C),$$

where $\mathbf{D} = Ra_m^{-1}\mathbf{I} + Ra_d^{-1}[(r-1)\frac{\mathbf{uu}}{|\mathbf{u}|} + |\mathbf{u}|\mathbf{I}]$

with $Ra_m = \frac{K \Delta \rho^* g H}{\mu \phi D_m}$, $Ra_d = \frac{H}{\alpha_t}$, and $r = \frac{\alpha_l}{\alpha_t}$

molecular Ra dispersive Ra dispersivity ratio

Note: generally $\alpha_l \gg \alpha_t$ ($r = 10$ in our most DNS)

- **Temporal discretization**
  Semi-implicit RK3
- **Spatial discretization**
  Fourier-Chebyshev-tau

Flux: molecular diffusion flux

$$F = \left.\left\langle \overline{\frac{\partial C}{\partial z}} + \frac{Ra_m}{Ra_d}\overline{|u|\frac{\partial C}{\partial z}} \right\rangle\right|_{z=1}$$

$$= F_m + F_d$$

dispersive flux

DNS Results (1): one-sided system ($Ra_m = 50000$)

DNS at $Ra_m = 50000$ demonstrating the effect of anisotropic mechanical dispersion on the convective pattern and flux (recall: $r \sim 10$ in advection dominated systems)

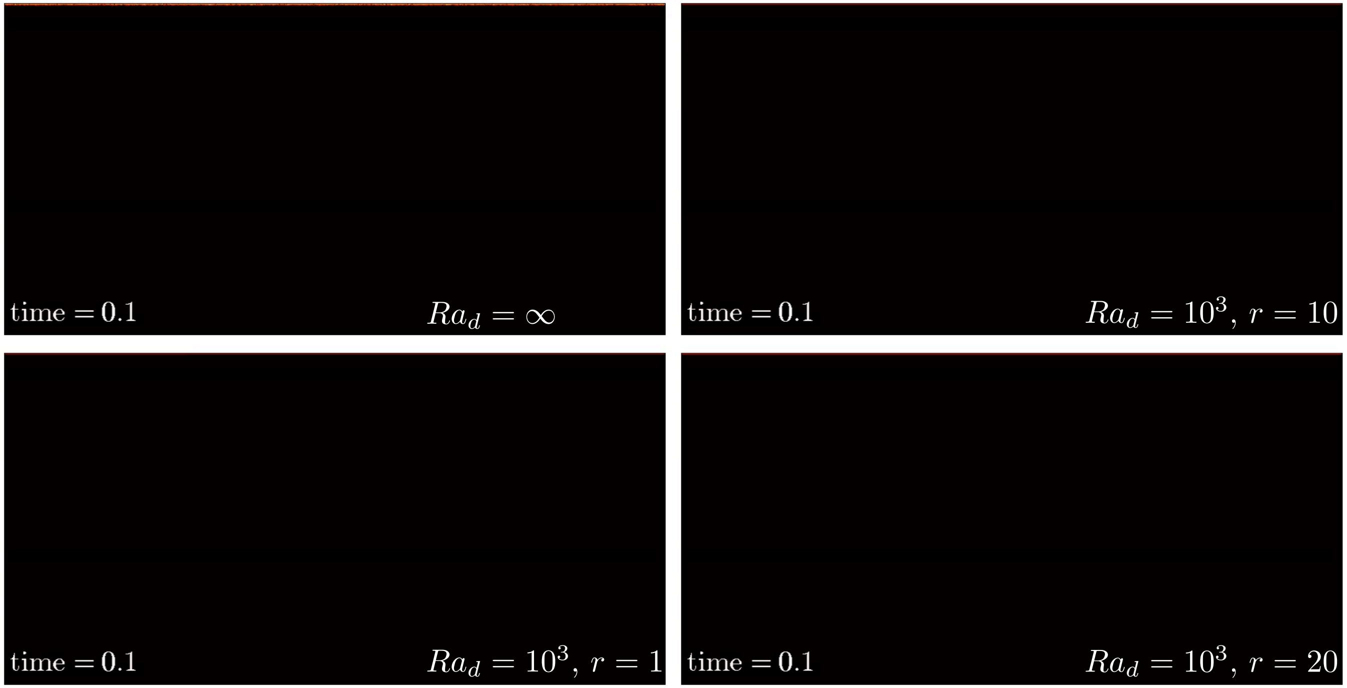

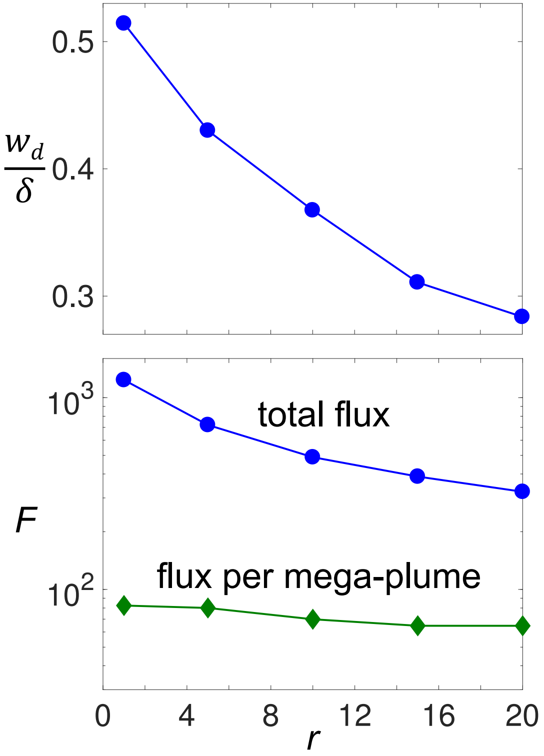

- Dispersion *coarsens* the convective pattern
- Introducing anisotropy, $r > 1$, makes the pattern *asymmetric* and *reduces* the overall convective flux

Asymmetry ratio: w_d/δ
where w_d is the plume width

DNS Results (2): two-sided system ($Ra_m = 20000$, $r \equiv 10$)

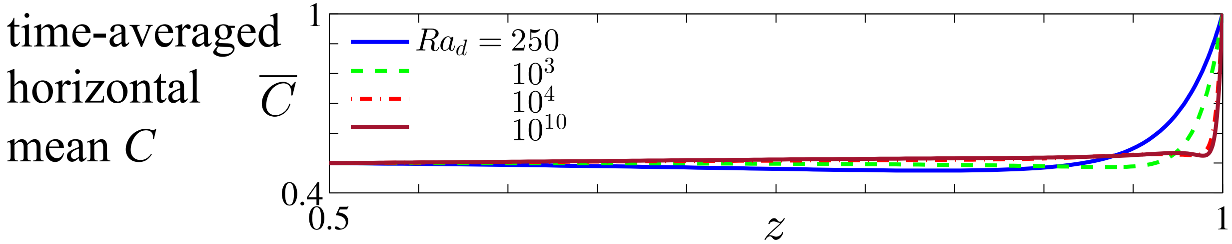

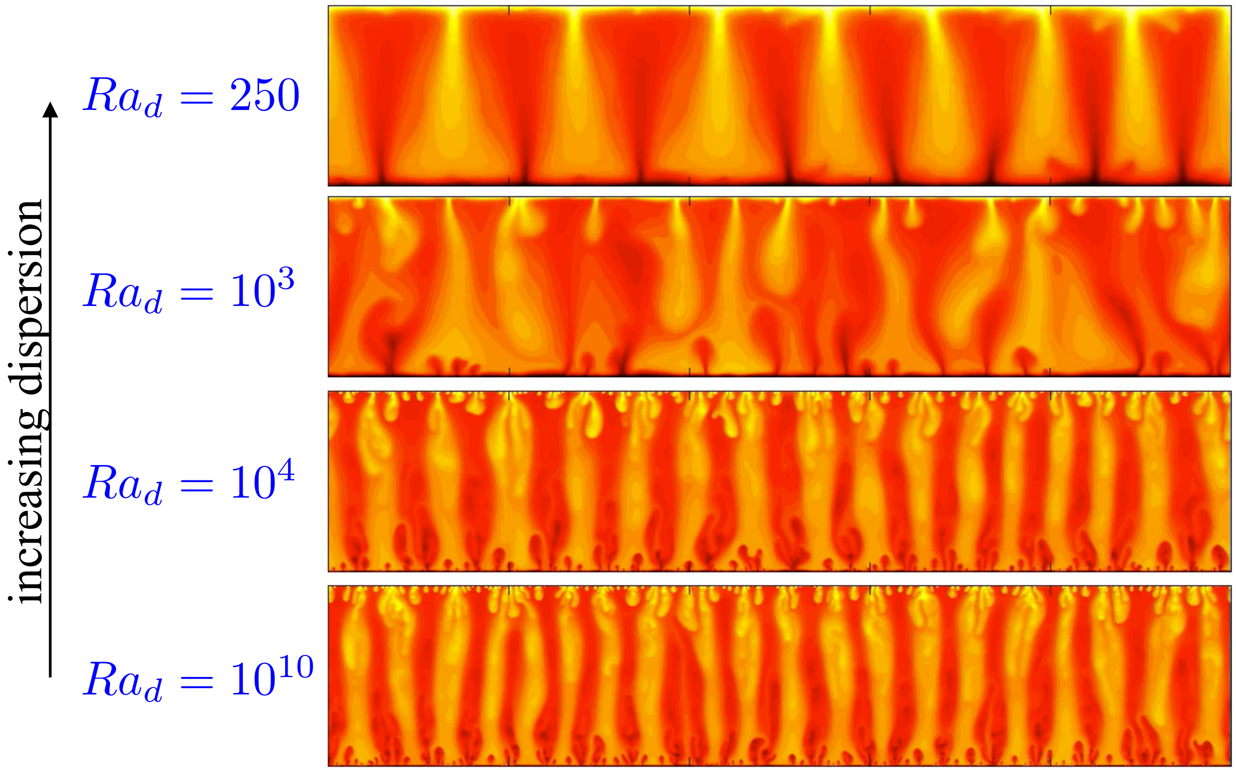

- Mechanical dispersion *thickens* the boundary layer and *coarsens* the convective flow pattern

Fan flow
strong dispersion

Columnar flow
weak dispersion

Note: videos are played in the same diffusion time rate

DNS Results (3): two-sided system ($Ra_m = 20000$, $r \equiv 10$) (cont'd)

Flux

$$F_m = \langle \partial_z \overline{C}|_{z=1} \rangle$$

$$F_d = \left\langle \frac{Ra_m}{Ra_d} \overline{|u|\partial_z C} \right\rangle \Big|_{z=1}$$

Inter-plume spacing

Mean (buoyancy) vertical velocity

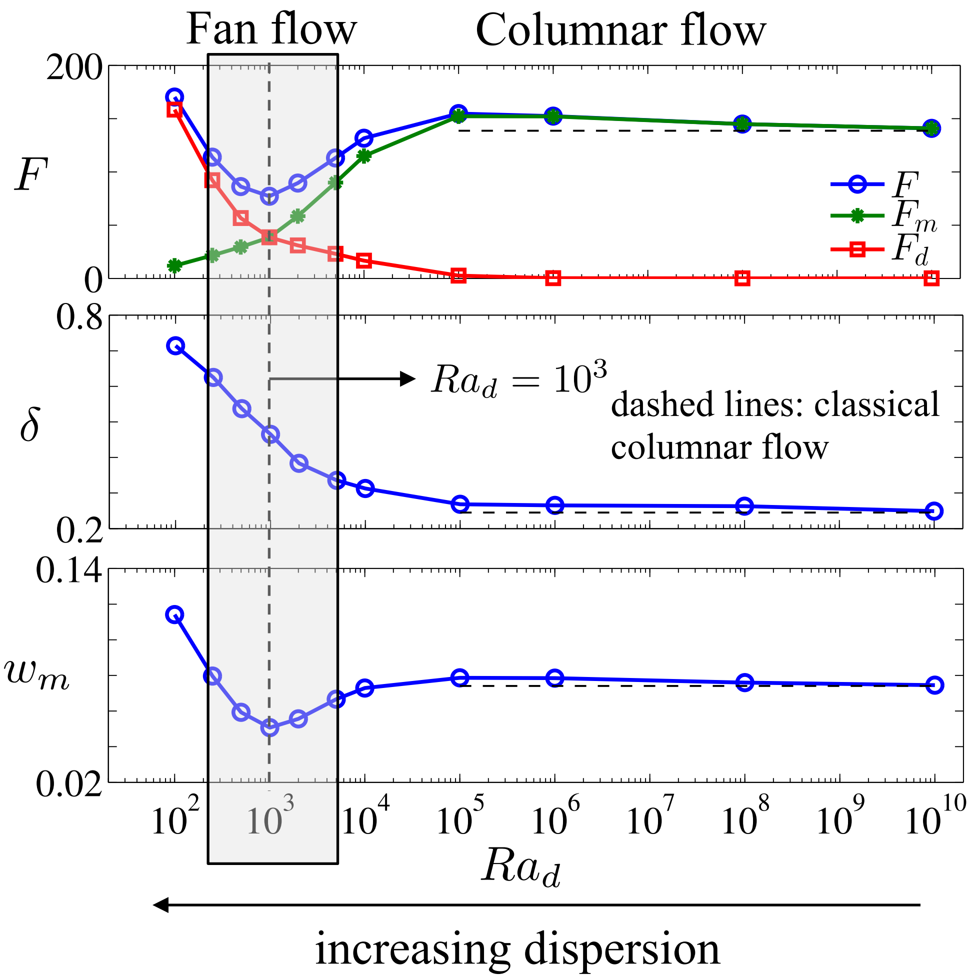

Fan flow

Columnar flow

$Ra_d = 10^3$

dashed lines: classical columnar flow

increasing dispersion

Note: in nature, $10^2 \lesssim Ra_d \lesssim 10^5$

- Moderate mechanical dispersion *reduces* the convective flux
- Increased mechanical dispersion *coarsens* the convective flow pattern

DNS Results (4): two-sided system ($Ra_d = 1000$, $r \equiv 10$)

time-averaged horizontal mean C

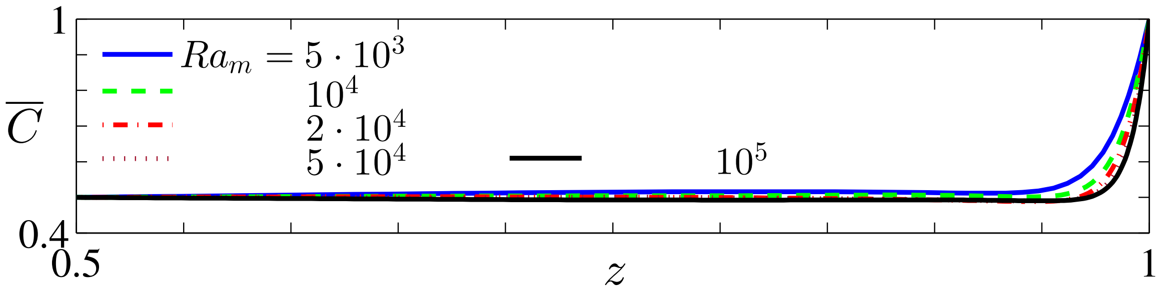

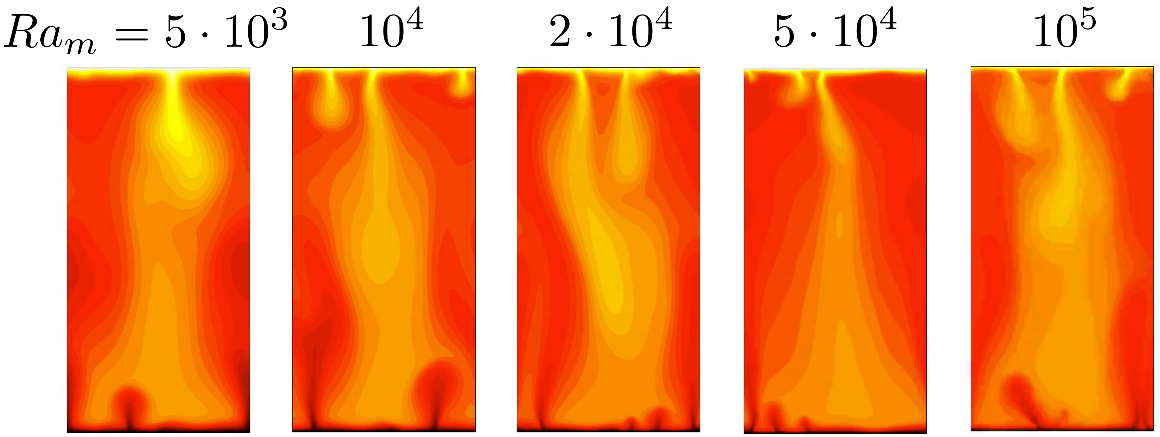

- The flow pattern (i.e. the statistical concentration field) is *determined* by Ra_d as $Ra_m \rightarrow \infty$

Note: videos are played in the same diffusion time rate

DNS Results (5): two-sided system ($Ra_d = 1000$, $r \equiv 10$) (cont'd)

Flux

$$F_m = \left\langle \partial_z \overline{C} \big|_{z=1} \right\rangle$$

$$F_d = \left\langle \frac{Ra_m}{Ra_d} \overline{|u| \partial_z C} \right\rangle \Bigg|_{z=1}$$

Inter-plume spacing

Mean (buoyancy) vertical velocity

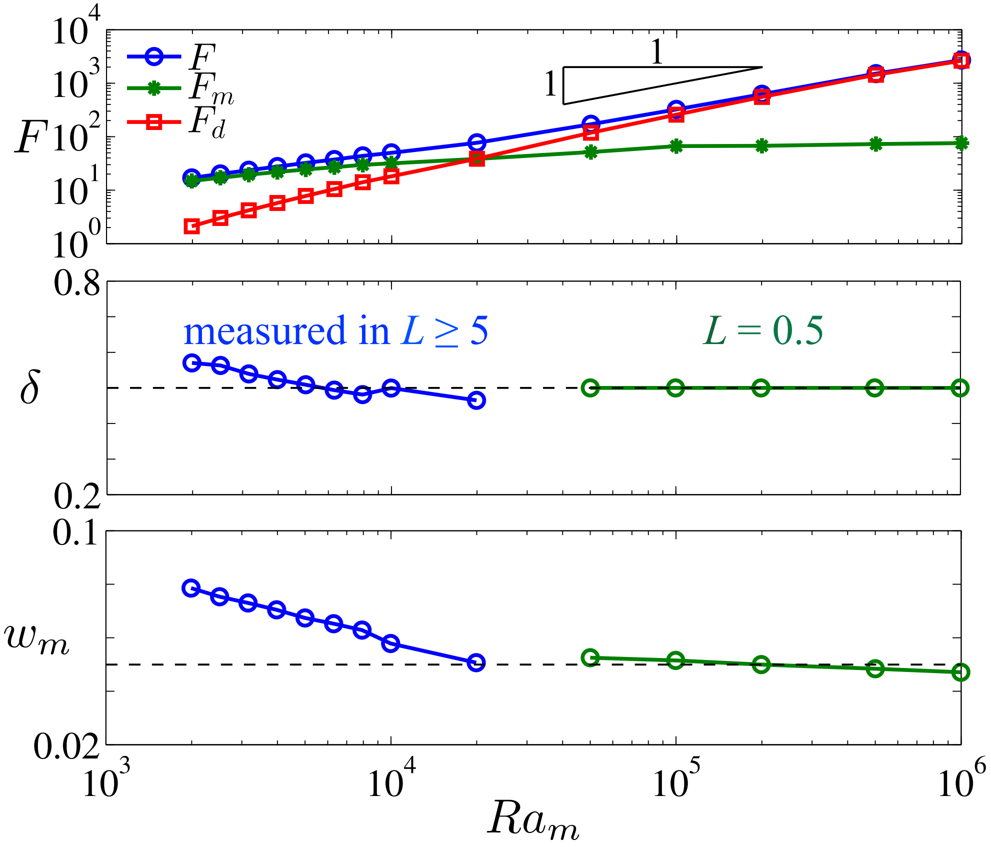

- The flow pattern (i.e. the statistical concentration and buoyancy velocity fields) is determined by Ra_d as $Ra_m \to \infty$, but the flux is predominantly controlled by Ra_m

Discussion: effect of mechanical dispersion on convection

$$\mathbf{D} = \frac{1}{Ra_m}\mathbf{I} + \frac{1}{Ra_d}\left[(r-1)\frac{\mathbf{uu}}{|\mathbf{u}|} + |\mathbf{u}|\mathbf{I}\right]$$

For fixed Ra_d and r, as $Ra_m \rightarrow \infty$,

$$\mathbf{D} \rightarrow \frac{1}{Ra_d}\left[(r-1)\frac{\mathbf{uu}}{|\mathbf{u}|} + |\mathbf{u}|\mathbf{I}\right].$$

- The system is only controlled by Ra_d for fixed $r \Longrightarrow$ the statistical concentration field C and buoyancy velocity $\mathbf{u}$ become independent of Ra_m

Moreover, as $Ra_m \rightarrow \infty$,

determined by Ra_d

$$F = \left\langle \overline{\frac{\partial C}{\partial z}} + \frac{Ra_m}{Ra_d}\overline{|u|\frac{\partial C}{\partial z}} \right\rangle\Bigg|_{z=1} \approx \left\langle \frac{Ra_m}{Ra_d}\boxed{\overline{|u|\frac{\partial C}{\partial z}}} \right\rangle\Bigg|_{z=1} \sim c(Ra_d)\cdot Ra_m^1$$

- The flux scales as $F \sim c(Ra_d) \cdot Ra_m^1$, while Ra_d determines the prefactor c

Discussion: effect of mechanical dispersion on convection (cont’d)

Flow direction isotropic $\mathbf{D}$ anisotropic $\mathbf{D}$ $(\alpha_l/\alpha_t = 10)$

Columnar flow *without* considering mechanical dispersion

Fan flow *after* considering mechanical dispersion

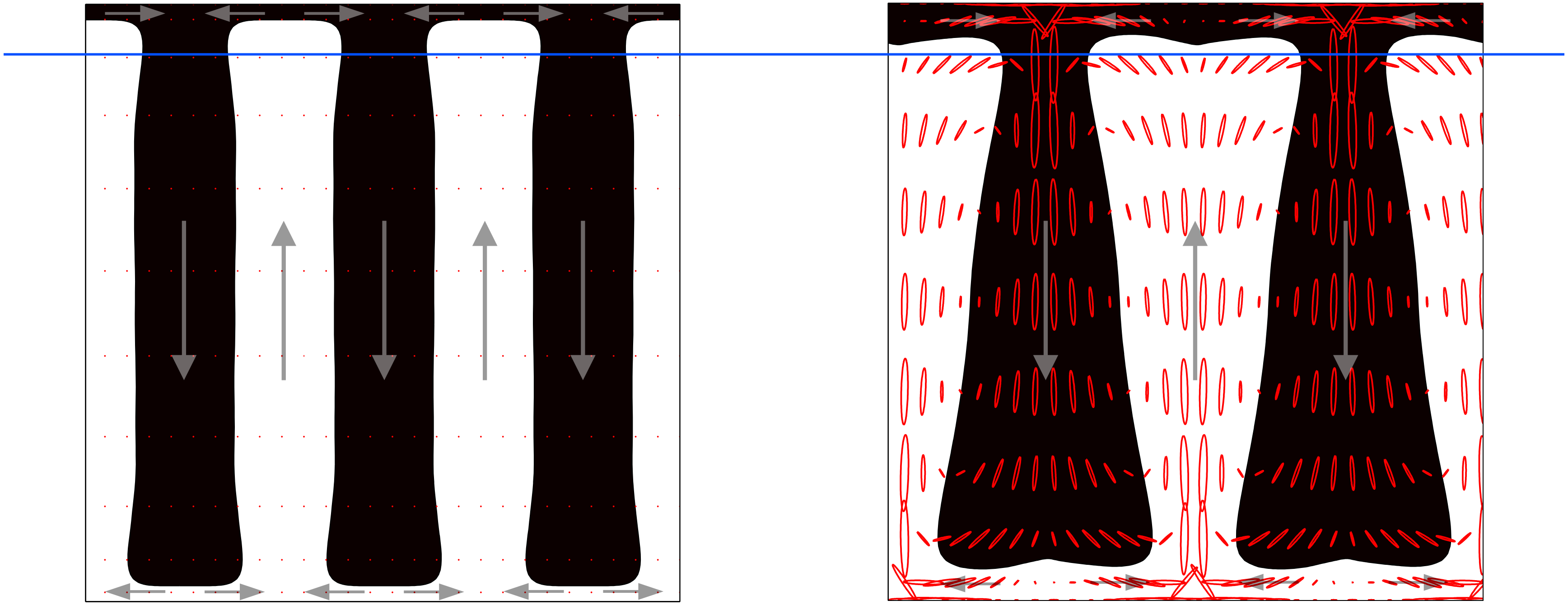

- Anisotropic hydrodynamic dispersion breaks the symmetry of the columnar structure

Conclusions

1) **Convection in porous media is significantly affected by the dispersive Rayleigh number $Ra_d = H/\alpha$ at large molecular Rayleigh number Ra_m**
2) **As $Ra_m \to \infty$, the convective flow pattern is *determined* by Ra_d, while the flux $F \sim c(Ra_d) \cdot Ra_m$ (which is also observed in experiments)**
3) **The inherent anisotropy of mechanical dispersion breaks the symmetry of the columnar flow structure and leads to a reduction of the transport flux at moderate Ra_d**
4) **Our numerical results are consistent with the experimental observations**

In experiments, increasing the grain size *d* leads to a larger Ra_m but also enhances the dispersion, which coarsens the convective pattern

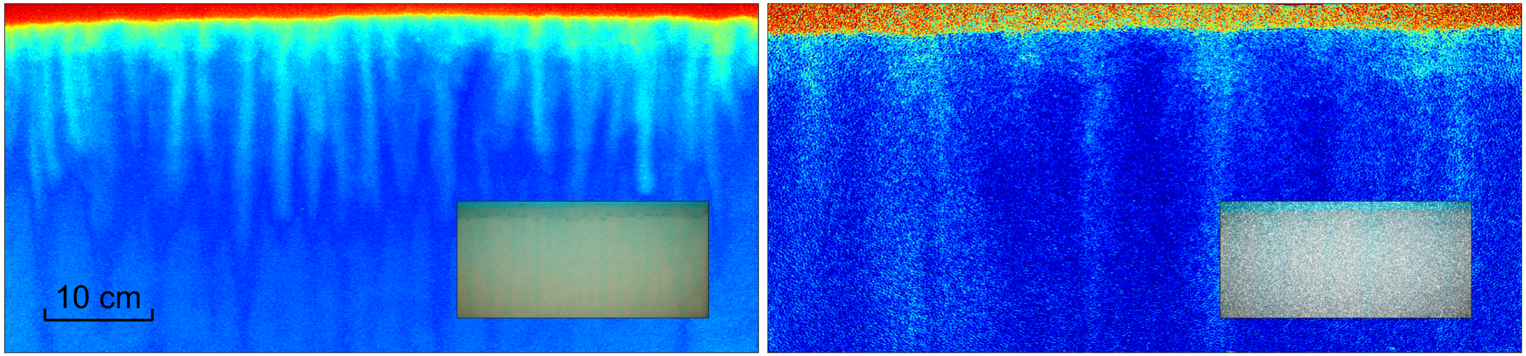

0.8mm glass bead, $Ra_m = 1.4 \cdot 10^4$ (19 plumes) 3mm glass bead, $Ra_m = 2.1 \cdot 10^5$ (9 plumes)

Publications

- B. Wen, K. W. Chang, M. Hesse. 201X Rayleigh-Darcy convection with hydrodynamic dispersion, in revision for *Physical Review Fluids*.
- L. Yu, B. Wen, M. Hesse, D. DiCarlo. 201X Scaling of solutal convection in porous media, in revision for *Geophysical Research Letters*.

Thanks!